

# Identification and *In Silico* Characterisation of Differentially Expressed *Aeromonas hydrophila* Induced Proteins from The Muscle of Indian Major Carp - *Gibelion catla* (Hamilton, 1822)

Madina Praveena<sup>1</sup>, Anusha N<sup>2</sup>, Aishwarya K<sup>3</sup>, Ch Gulabi Rao<sup>4</sup>, Ratnakala M<sup>5</sup>

<sup>1,2,3,5</sup>Dept. of Zoology, College of science and technology, Andhra University, Visakhapatnam, Andhra Pradesh, India

<sup>4</sup>Dept. of Biotechnology, Dr. V. S. Krishna Govt. Degree College, Visakhapatnam, Andhra Pradesh, India

\*Corresponding author: Anusha Nutangi, anushanutangi333@gmail.com

## Abstract

Fish are significant, as they provide essential nutrients that enhance growth and health in both humans and animals. Overcrowding and environmental issues, including inadequate water quality and various stressors, can lead to disease outbreaks in farmed fish, resulting in considerable losses for farmers. Several species of *Aeromonas* are recognized as severe pathogenic bacteria affecting shellfish and fish. Understanding the molecular pathways influenced by *A. hydrophila* infection is crucial for clarifying its impacts and addressing gaps in current research. This study focused on identifying and characterizing differentially expressed proteins in the muscle of *G. catla* related to *A. hydrophila* infection. Protein measurement revealed that protein concentrations in muscle increased with infection dosage up to 500  $\mu$ L/L ( $13.22 \pm 0.4$  mg/g FW), followed by a decline with further increase. Comparative proteome analysis via SDS-PAGE revealed that two peptides with molecular weights of 35 and 28 kDa were differentially expressed in fish exposed to *A. hydrophila* at dosages of 750 and 1000  $\mu$ L/L. These proteins were identified as cathepsin and mitochondrial NADH dehydrogenase subunit 2. The physicochemical characterization revealed that the cathepsin and mt NADH dhf-2 proteins were acidic, with pI values of 5.58 and 5.70. The secondary structure indicated that random coils and alpha helices were predominant in cathepsin and mt NADH dhf-2, with respective percentages of 52.40% and 45.90%. Additionally, homology modeling revealed that C8he9A and C5xtbN are the most appropriate templates for cathepsin and mt NADH dhf-2. This research demonstrated that the predicted 3D models of cathepsin and mt NADH dhf-2 were reliable and coherent.

**Keywords:** *A. hydrophila*, *G. catla*, Proteome, SDS-PAGE, Cathepsin, mt NADH dehydrogenase flavoprotein.

## INTRODUCTION

Fish serves as essential for supplying necessary nutrients to both animals and people, thereby promoting health and growth. Systematic fish consumption aids in the prevention of cardiovascular illnesses.<sup>1</sup> Fish provides vital nutrients, including high-quality proteins and lipids, earning it the label of "nutritious food for the impoverished".<sup>2</sup> Moreover, fish serves as a nutritional resource and contributes to the prevention of numerous diseases in people.<sup>3</sup> Consequently, aquaculture is a vital business defined by the cultivation of diverse marine and freshwater fish, which enhances global annual production. Fish are generally farmed in restricted settings like ponds or net enclosures, with efforts focused on increasing output per unit area. Chinabut and Puttinawarat<sup>4</sup> state that aquaculture rapidly progressed from big systems to semi-intensive, intensive, and super-intensive systems. Unfortunately, overcrowding and environmental challenges, such as inadequate water quality and various stresses, may result in disease outbreaks in cultured fish. Moreover, fish in cultured ecosystems generally exhibit suboptimal physiological circumstances and demonstrate increased vulnerability to diseases.<sup>5</sup> Since bacterial diseases can lead to large-scale production losses and major economic consequences, they present formidable obstacles in aquaculture. Numerous species of *Vibrio* and *Aeromonas* are identified as harmful bacteria that impact shellfish and fish.<sup>6</sup> As a result, the aquaculture industry faced considerable challenges stemming from intensive growing practices and bacterial diseases, leading to substantial losses for farmers.

*Aeromonas hydrophila*, a motile Gram-negative bacillus, induces motile *Aeromonas* septicemia and various kinds of diseases in humans and animals.<sup>7</sup> The manifestations of an *Aeromonas* infection encompass skin and fin rot, haemorrhages, ulcers, abdominal distension, exophthalmia, congestion, and fin rot. Furthermore, examining an organism's reaction to a stressful event comprises two categories of responses: direct responses,

which influence biochemical and metabolic functions, and indirect responses, which impact the food chain, habitat accessibility, and behavioural modifications.<sup>8</sup> These factors hinder growth, elevate farm mortality and morbidity, induce food insecurity, diminish revenue, escalate production costs, and may transmit to humans.<sup>9</sup> The identification and analysis of biomarkers, particularly in fish, is acknowledged as an effective method for understanding the condition of stressed ecosystems and their interactions with aquatic organisms.<sup>10</sup> In this context, fish biochemical measures have emerged as valuable diagnostic instruments and potential stress indicators.<sup>11</sup> These metrics are essential for assessing the general health of fish and the severity of stress-induced responses. Therefore, comprehending the molecular pathways affected by *A. hydrophila* infection is essential for elucidating its effects and addressing the deficiencies in existing research.

*Gibelion catla*, a member of the Cyprinidae family, also known as Indian carp or catla, is a species experiencing fast expansion and garnering market attention.<sup>12</sup> It is located in Bangladesh, Nepal, India, Pakistan, Myanmar, Sri Lanka, and China. This species is native to North India and has lately been introduced to Peninsular India. The *G. catla* fish species holds considerable ecological significance by predominantly feeding on algae and plankton, thus regulating the population density of these microscopic organisms.<sup>13</sup> *G. catla* enhances overall environmental health and promotes biodiversity by mitigating severe eutrophication and indirectly increasing water quality.<sup>14</sup> Catla possesses significant economic and cultural importance, in addition to being an excellent choice for commercial fishing in South Asia, owing to its enormous size and high-quality flesh.<sup>15</sup> Additionally, catla is a rich source of healthy fats, including omega fatty acids like docosahexaenoic acid, arachidonic acid, and eicosapentaenoic acid, which our bodies cannot produce and must be obtained from food. Furthermore, the literature review revealed a lack of comprehensive evidence regarding the effects of *A. hydrophila* infection on proteome expression. Hence, this study concentrated on the identification and *in silico* characterization of differentially expressed proteins in the muscle tissue of *G. catla* in connection to *A. hydrophila* infection.

## MATERIALS AND METHODS

### Collection and acclimatisation of fish samples

Live healthy and young *G. catla* fish samples, weighing  $150\pm20$  g, were collected at a private farm (Long:  $83^{\circ}10' 14.88''$  to  $83^{\circ}11' 6.72''$  E; Lat:  $17^{\circ}40' 23.52''$  to  $17^{\circ}45' 57.6''$  N) in K. Kotapadu village, Visakhapatnam, Andhra Pradesh, India. The live samples were carried to the lab in sterile zip pouches with pond water and maintained under regulated conditions. All fish were kept for two weeks to acclimatise to the laboratory environment. Fish were maintained in  $50 \times 30 \times 40$  cm plastic containers with aerated, dechlorinated tap water.

### Experimental design

A study was performed to assess the possible biotic stress effect of *A. hydrophila* infection on the physiological responses and proteomic responses in *G. catla*. The experiment was carried out with five experimental groups. The first group of fish was grown under normal conditions without *A. hydrophila* infection and is referred to as the control group. While, the 2<sup>nd</sup>, 3<sup>rd</sup>, 4<sup>th</sup>, and 5<sup>th</sup> experimental groups fish treated with the  $10^6$  CFU/mL *A. hydrophila* culture with increasing dosages of 250, 500, 750, and 1000  $\mu$ L/L respectively. All the treatment groups were administered 3 gm of feed at 12-hour intervals. The water temperature and pH were calibrated at 25°C and 5.6 respectively. The photoperiod is established at 12 hr of light and 12 hr of darkness. Aerators were affixed to tubs to enhance aeration. Every day, half of the water in the tub was replaced with fresh, dechlorinated tap water, and the fish were maintained for two weeks in all the experimental groups. Following 14 days of exposure, fish were collected from each group and dissected the tissue for proteomic analysis. (Figure 1)



**Figure 1: Experimental groups of fishes**

#### **Extraction and Estimation of total protein content**

The total protein content in the muscular tissues of *G. catla* from all experimental groups was extracted using 0.1 M phosphate buffer (pH 7.4). 2 gm of muscle tissue from each experimental group were independently homogenised with 5 ml of phosphate buffer. The homogenate was centrifuged for ten minutes at 4°C and 14,000 rpm. The supernatant was collected and utilised for protein quantification by Lowry et al., method<sup>16</sup>. To ascertain protein content, 4 ml of a freshly prepared alkaline solution was added to 1 ml of protein extract and incubated for 15 minutes. Subsequently, 0.5 ml of Folin-Ciocalteau reagent was added and incubated for 30 minutes. After incubation, the colour intensity was quantified by measuring the absorbance at 660 nm. The total protein concentration in the sample was determined by comparing the optical densities of the test sample with the BSA calibration curve.

#### **Protein separation by SDS PAGE**

The separation of proteins from all the crude extracts of *G. catla* were performed by SDS-PAGE according to the methodology of Sambrook and Russell.<sup>17</sup> The crude protein sample was mixed in the sample loading buffer at a 1:3 v/v ratio, and it was heated to 95°C for 10 minutes, subsequently cooled. The sample was then subjected to SDS-PAGE alongside a parallel run of protein markers with molecular weights ranging from 250-10 KDa. The Laemmli<sup>18</sup> method was utilised to prepare a 12% resolving gel and a 5% stacking gel. The electrophoresis was initially carried out at 100 V. Followed by electrophoresis, the gel was stained for overnight using 0.5% Coomassie Brilliant Blue R-250 and then destained until the background was clear. The gel was examined to identify the protein bands that were differentially expressed among all the treatment groups. The differentially expressed peptide gel bands from the *A. hydrophila* infected fish were extracted from the gel by suspending them in elution buffer and precisely crushing the mixture. Then the solution was centrifuged at 10000 rpm for 10 minutes at 4°C and the supernatant containing the eluted peptide fraction was collected.

#### **Identification of extracted peptides**

For identification and molecular weight determination, the eluted peptide fraction was analysed through peptide mass fingerprinting using MALDI-TOF/MS. For PMF, 0.5 µL of the eluted peptide was applied to a matrix that contained saturated α-cyano-4-hydroxycinnamic acid that had been made with 50% acetonitrile and 5% trifluoroacetic acid. The mass spectrometric data of the digested protein sample was obtained using the ABI 4800 MALDI-TOF (Applied Biosystems, Foster City, CA). The spectral data were obtained in reflector mode across a mass range of 600-4500 Da. The generated mass spectrum was subjected to sequence database searches utilising MASCOT software. The MASCOT software analysis generated a score that indicated the likelihood of a true positive identification, with a minimum value of 50.

#### ***In silico* characterisation**

The identified peptides were characterised by predicting their physicochemical characteristics, secondary structure, tertiary structure, gene ontologies for their biological functions, and PPI networks. The FASTA sequences of the identified proteins were obtained from UniProt, a publicly available protein database at

[www.uniprot.org](http://www.uniprot.org).<sup>19</sup> The ProtParam server from Expasy was utilised to ascertain the physicochemical properties. The secondary structural components of the identified peptide were predicted utilising the SOPMA server. The 3D model was generated using the Phyre2 server.<sup>20</sup> Subsequently, the 3D model quality was assessed using the QMEAN scoring function and Ramachandran plot analysis using the PROCHECK server. The functional annotations of proteins were predicted by using DeepGoWeb server. Furthermore, the PPI networks were established using STRING analysis via PPI pairs with protein interaction values exceeding 0.4.

## RESULTS AND DISCUSSION

### Estimation of protein

Quantifying proteins in any organism is crucial for evaluating its physiological and metabolic condition, as protein levels directly correlate with health status. Table 1 displays the total protein content in fish grown under control and different dosages of *A. hydrophila* infection. From these results, the protein content in the fish of 0 (control), 250, 500, 750, and 1000  $\mu$ L/L *A. hydrophila* infected groups was found to be  $8.48 \pm 0.79$ ,  $10.95 \pm 0.26$ ,  $13.22 \pm 0.4$ ,  $11.98 \pm 0.13$ , and  $8.32 \pm 0.4$  mg/gmFW respectively. According to the present results, it was observed that the mean value of total protein content was significantly increased with the dosage of *A. hydrophila* infection up to 750  $\mu$ L/L. However, the fish infected with 1000  $\mu$ L/L *A. hydrophila* administration exhibited significantly decreased total protein content compared to the other infected groups. Furthermore, the protein content from the control group fish and 1000  $\mu$ L/L *A. hydrophila* infected fish exhibited almost similar values. The results of Tukey's HSD test demonstrated that the fish administered with *A. hydrophila* culture with increasing dosages, such as 0, 250, 500, and 750  $\mu$ L/L exhibited significantly increased total protein content with p-values less than 0.05 when compared to fish fed with control feed. But the fish infected with 1000  $\mu$ L/L *A. hydrophila* exhibited a very insignificant increase in total protein content with a p-value of 0.782. The Tukey's HSD results were presented in Table 2.

**Table 1: Total protein content in the fish administered with increasing dosages of *A. hydrophila* culture.**

S. No	A. hydrophila culture ( $\mu$ L/L)	Mean $\pm$ SD (mg/gmFW)	Std. Error	Variance	Range	Confidence level (95%)
1	0 (Control)	$8.48 \pm 0.79$	0.46	0.62	1.53	1.964
2	250	$10.95 \pm 0.26$	0.15	0.07	0.5	1.648
3	500	$13.22 \pm 0.4$	0.23	0.16	0.78	0.969
4	750	$11.98 \pm 0.13$	0.07	0.02	0.25	0.311
5	1000	$8.32 \pm 0.4$	0.23	0.16	0.8	1.002

**Table 2: Tukey's HSD analysis of the total protein content in fish administered with increasing dosages of *A. hydrophila* culture**

S. No.	Pairwise comparisons	Tukey's HSD	Q value	P value
1	T1 : T2	2.28	12.19	0.000
2	T1 : T3	4.61	24.66	0.000
3	T1 : T4	3.35	17.92	0.000
4	T1 : T5	0.30	1.62	0.782
5	T2 : T3	2.33	12.47	0.000
6	T2 : T4	1.07	5.73	0.005
7	T2 : T5	2.58	13.81	0.000
8	T3 : T4	1.26	6.74	0.009
9	T3 : T5	4.91	26.28	0.000
10	T4 : T5	3.65	19.53	0.000

T1- fish grown under normal condition without *A. hydrophila* (Control).

T2- fish treated with 250  $\mu$ L/L *A. hydrophila* culture

T3- fish treated with 500  $\mu$ L/L *A. hydrophila* culture

T4- fish treated with 750  $\mu$ L/L *A. hydrophila* culture

T5- fish treated with 1000  $\mu$ L/L *A. hydrophila* culture

Assessing physiological and metabolic conditions requires quantifying proteins in organisms, as protein levels directly correlate with health status. The current results indicate a significant enhancement in the protein levels of fish subjected to *A. hydrophila* exposure. The protein content in fish tissues exhibits minor variations during particular developmental phases of food restriction.<sup>21</sup> Adawayah<sup>22</sup> states that fish can have a protein concentration up to 20%. Dabhadé et al.,<sup>23</sup> indicated that most of the protein consumed by fish is absorbed and stored in muscle tissue. Previous studies by Satyalatha and Viveka<sup>24</sup> demonstrated that *A. liquefaciens* infection in *L. rohita* resulted in elevated protein levels in muscle tissue across various treatment groups. This suggests that the magnitude of secondary immune response was contingent upon repeated doses, with the  $10^{-6}$  dose identified as optimal for sensitizing the immune system. Similarly, studies of Karunasagar et al.,<sup>25</sup>, Lamers and Van Muiswinkel<sup>26</sup>, and Newman<sup>27</sup> found that different antigen preparations of motile aeromonas in fish considerably change the profile of biochemical components. Furthermore, they found muscle protein levels were significantly elevated at 6 hr (70.0 mg/mL) in fish receiving  $10^2$  CFU. In fish administered with  $10^5$  CFU, greater amount of protein was observed at 12 hr (70.68 mg/mL), and 24 hr (71.37 mg/mL). For fish administered with  $10^6$  CFU, the protein levels are remained constant from 1 hr (72.06 mg/mL) to 216 hr (72.06 mg/mL) when compared to controls. Begum<sup>28</sup> found that *L. rohita* had dose-dependent greater concentrations of muscle protein during aeromoniasis. Aeromoniasis causes significant physiological changes in test fish, including changes in muscle protein, suggesting that the fish are vulnerable to stress. However, as stated by Miyamoto<sup>29</sup> and Murty and Devi<sup>30</sup> a decrease in protein content may be the result of decreased metabolism. Das and Bhattacharya<sup>31</sup> suggest that a decline in protein synthesis could account for the low protein level, while proteolytic alterations could lead to an increase in amino acids. Neilson<sup>32</sup> proposed that the metabolic use of ketoacids for gluconeogenesis and enzyme detoxification could be the cause of a noticeable drop in total protein under both high and low doses. Veeraiah and Durga Prasad<sup>33</sup> and Durairaj and Selvarajan<sup>34</sup> also suggested that *O. mossambicus* and *L. rohita* exposed to pollutants showed a decrease in protein levels in their gill, liver, muscle, and brain tissues which are used for energy under stress.

### Protein separation by SDS-PAGE

The analysis of the *G. catla* muscle proteome from all the experimental groups was conducted utilizing SDS polyacrylamide gel electrophoresis, revealing that the molecular weights of the expressed proteome span from 20 to 250 kDa. Moreover, the majority of the protein bands exhibit high and medium molecular weights. The current study on comparative muscle proteome analysis showed that most of the protein bands were the same in all the treatment groups (Figure 2). However, two protein bands were additionally found in fish exposed to *A. hydrophila* with 750 and 1000  $\mu$ L/L dosages, suggesting that these proteins were expressed at significantly high levels, with molecular weights recorded at 35 and 28 kDa. These two protein bands derived from the 750 and 1000  $\mu$ L/L *A. hydrophila* exposed fish were chosen for MALDI-TOF/MS analysis to facilitate the identification of the proteins.

Proteins act as the primary regulators of metabolic functions, promoting growth and development, their synthesis experiences substantial changes in reaction to environmental stress. Differentially expressed proteins were linked to a wide range of cellular and physiological functions, including ion balance, redox equilibrium, osmoregulation, as well as energy and carbohydrate metabolism. Prior research including Dawar et al.,<sup>35</sup>, Ali et al.,<sup>36</sup> and Canellas et al.,<sup>37</sup> has indicated that the proteome composition of skin mucus from fish existing in diverse environments is consistently distinctive and intriguing. Ali et al.,<sup>36</sup> observed that following an *A. hydrophila* infection in *Ctenopharyngodon idella*, a total of 126 proteins were found to be differently expressed, comprising 89 upregulated and 37 downregulated. Similarly, Lu et al.,<sup>38,39</sup> documented an elevated level of complement proteins in the gill and skin of *D. rerio* when challenged with *Citrobacter freundii* and *A. hydrophila*. Zaccone et al.,<sup>40</sup> found that the 20S proteasome complex in rainbow trout, which consists of  $\alpha$  and  $\beta$  subunits, interact with *A. salmonicida*, suggesting that they have a role in fighting against bacterial infections. Dash et al.,<sup>41</sup> found that Japanese flounder when exposed to *Edwardsiella tarda*, their kidneys

had higher levels of cathepsin L, which also reduced the bacterial growth. However, Japanese flounder liver showed an upregulation of cathepsin D, indicating their function as an immune system against *E. tarda*.<sup>42</sup> Ali et al.,<sup>36</sup> identified that the skin mucus of *A. hydrophila* infected *C. idella* upregulated immune related proteins including annexin, calpain, cathepsin, complement proteins, heat shock proteins, intelectin, lysozyme, 26S proteosome, and transferrin.

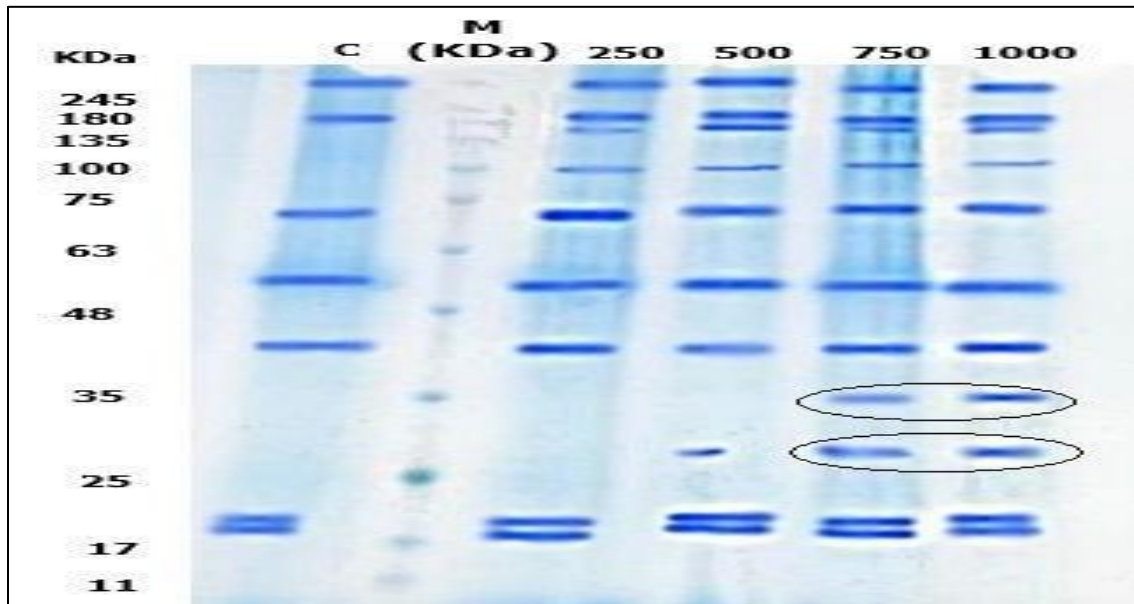


**Figure 2: Protein profiling of *Gibelion catla* muscle proteome under control and *A. hydrophila* exposed conditions by SDS-polyacrylamide gel.**

#### Protein identification

Peptide mass fingerprinting represents a systematic approach for the identification of unknown proteins through the analysis of their peptide masses. This technique relies extensively on the availability of high-quality protein databases.<sup>43</sup> In this research, the PMF results showed that the protein bands at 35 and 28 kDa matched the cathepsin and mitochondrial NADH dehydrogenase flavoprotein-2 (mt NADH dhf-2) respectively. The mass spectrum data also show that *G. catla* cathepsin and mt NADH dhf-2 are most similar to their corresponding proteins in *Labeo rohita* (Accession number A0A498MHB7) and *Parambassis ranga* (Accession number A0A6P7K3W8), with predicted identity scores of 82.3 and 87.4% respectively. Figures 3 and 4 present the mass spectra for the protein bands at 35 and 28 kDa respectively. Table 3 presents a summary of the protein identification results from peptide mass fingerprinting.

**Table 3: Identification result of the differentially expressed proteins by peptide mass fingerprinting**

Source Organism	Protein Gel Band	Max. homology (Protein name)	Best match organism	Expt/Theor. Mw (KD)	Score (Ms)	Accession No.
<i>G. catla</i>	35 kDa	Cathepsin	<i>Labeo rohita</i>	35/33	82.3	A0A498MHB7
<i>G. catla</i>	28 kDa	mt NADH dehydrogenase flavoprotein-2	<i>Parambassis ranga</i>	28/25	87.4	A0A6P7K3W8

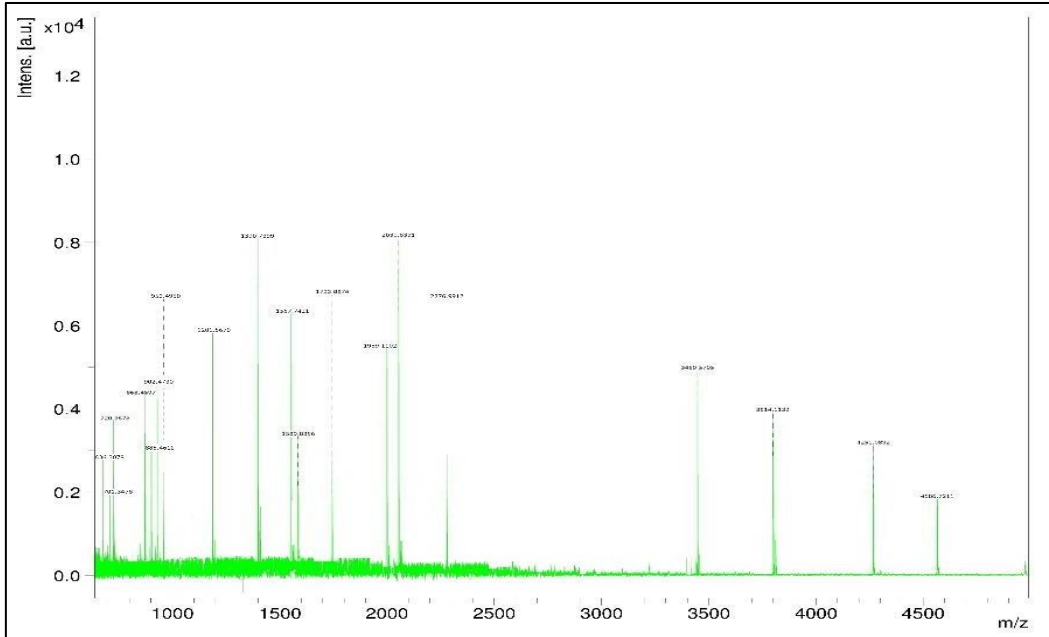


**Figure 3: MALDI-TOF/MS spectrum of 35 KDa protein**

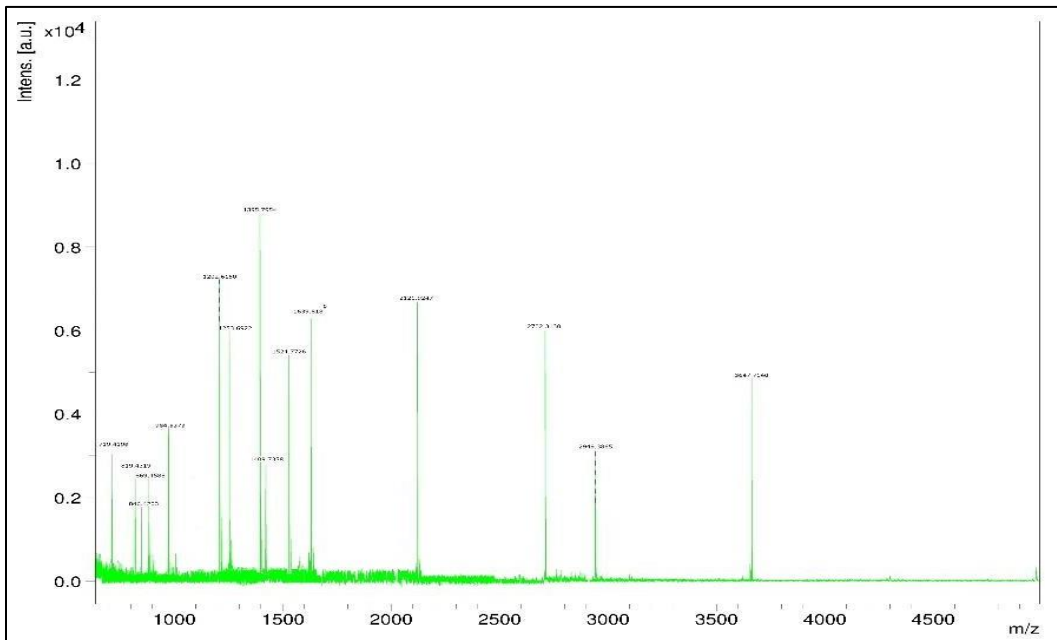


**Figure 4: MALDI-TOF/MS spectrum of 28 KDa protein**

## *In silico* characterisation

## Physicochemical characterisation

Cathepsin and mt NADH dhf-2 proteins consists of 334 and 244 amino acids respectively, with estimated molecular weights of 36587.16 and 26891.92 Da. Table 4 presents the physicochemical properties of Cathepsin and mt NADH dhf-2 proteins. The isoelectric points (pI) for cathepsin and mt NADH dhf-2 proteins were found to be 5.58 and 5.70 respectively which indicates both the proteins were acidic. The pI represents the precise value at which a molecule achieves electrical neutrality, which is characterised by an equal distribution of negative and positive charges. The protein's immobility at the pI makes it a useful component in the formulation of buffer system for isoelectric focus separation. The extinction coefficients of

cathepsin and mt NADH dhf-2 proteins were  $82360\text{ M}^{-1}\text{cm}^{-1}$  and  $14815\text{ M}^{-1}\text{cm}^{-1}$  when all pairs of cysteine residues are converted into cystines. Furthermore, upon reduction of all cystine residues, the extinction coefficients of cathepsin and mt NADH dhf-2 were  $81360\text{ M}^{-1}\text{cm}^{-1}$  and  $14440\text{ M}^{-1}\text{cm}^{-1}$  respectively. The highest extinction coefficient represents an elevated concentration of Trp and Tyr. Cathepsin and mt NADH dhf-2 proteins were shown to have instability indices of 33.92 and 54.93 respectively. The protein instability index indicates the stability of a protein under laboratory conditions. Guruprasad et al.,<sup>44</sup> state that a protein is deemed stable if its instability index is less than 40 and that a number greater than 40 suggests possible protein instability. Zaccaria et al.,<sup>45</sup> demonstrated that small elements located near N-terminus of a protein affect its stability, thereby influencing its longevity. Rogers et al.,<sup>46</sup> demonstrated that proteins with a half-life of less than 5 hours exhibited an instability index exceeding 40, while those with a half-life greater than 16 hours had an instability index below 40.

Cathepsin and mt NADH dhf-2 proteins exhibited half-life of approximately 30 hours in mammalian reticulocytes under invitro conditions, while their half-lives exceed 20 hours in yeast and 10 hours in *E. coli*. The protein sequences of cathepsin and mt NADH dhf-2 proteins were found to have aliphatic indices of 67.16 and 84.34 respectively. The aliphatic index of these proteins reflects their stability across different temperatures. The aliphatic index measures the proportion of a protein's volume that is occupied by aliphatic side chains, particularly those derived from the amino acids such as alanine, valine, isoleucine, and leucine. It is considered a valuable factor in improving the thermal stability of globular proteins. Proteins with a high aliphatic index are anticipated to demonstrate stability over a wide range of temperatures. The diminished thermal stability over a wide range of temperatures suggests a structure characterised by increased flexibility.<sup>47</sup> The GRAVY indices for cathepsin and mt NADH dhf-2 proteins were calculated to be -0.289 and -0.176 respectively. The negative GRAVY suggests that proteins exhibit a polar and hydrophilic nature, resulting enhanced interactions with water.<sup>48</sup> The results indicate that ionisable amino acids located on the protein surface, accessible to water, predominantly affect the pI of proteins. Table 5 presents the amino acid composition of cathepsin and mt NADH dhf-2 proteins.

**Table 4: Physicochemical characteristics of cathepsin and mt NADH dhf-2 proteins**

Parameter		Cathepsin	mt NADH dhf-2
Total no. of amino acids		334	244
Molecular weight		36587.16 Da	26891.92 Da
pI		5.58	5.70
Positively charged residues		26	23
Negatively charged residues		34	28
Extinction coefficient	Cys oxidised	$82360\text{ M}^{-1}\text{cm}^{-1}$	$14815\text{ M}^{-1}\text{cm}^{-1}$
	Cys reduced	$81360\text{ M}^{-1}\text{cm}^{-1}$	$14440\text{ M}^{-1}\text{cm}^{-1}$
Instability index		33.92	54.93
Aliphatic index		67.16	84.34
GRAVY		-0.289	-0.176
Half-life	In mammalian reticulocytes	30 hours	30 hours
	In yeast	>20 hours	>20 hours
	In <i>E. coli</i>	>10 hours	>10 hours
Formula		$\text{C}_{1625}\text{H}_{2434}\text{N}_{438}\text{O}_{486}\text{S}_{22}$	$\text{C}_{1194}\text{H}_{1887}\text{N}_{325}\text{O}_{353}\text{S}_4$

**Table 5: Amino acid composition of cathepsin and mt NADH dhf-2 proteins**

Amino acid	Cathepsin		mt NADH dhf-2	
	No. of Residues	% of Residues	No. of Residues	% of Residues
Ala (A)	23	6.9	19	7.8

Arg (R)	10	3.0	13	5.3
Asn (N)	18	5.4	10	4.1
Asp (D)	18	5.4	12	4.9
Cys (C)	16	4.8	6	2.5
Gln (Q)	11	3.3	9	3.7
Glu (E)	16	4.8	16	6.6
Gly (G)	36	10.8	17	7.0
His (H)	9	2.7	6	2.5
Ile (I)	16	4.8	18	7.4
Leu (L)	20	6.0	18	7.4
Lys (K)	16	4.8	10	4.1
Met (M)	6	1.8	8	3.3
Phe (F)	13	3.9	10	4.1
Pro (P)	20	6.0	22	9.0
Ser (S)	28	8.4	11	4.5
Thr (T)	12	3.6	16	6.6
Trp (W)	11	3.3	1	0.4
Tyr (Y)	14	4.2	6	2.5
Val (V)	21	6.3	16	6.6

### Secondary structure

The secondary structure of cathepsin comprises 25.75% alpha helices, 15.27% extended strands, 6.59% beta turns, and 52.40% random coils. The secondary structure of mt NADH dhf-2 protein is composed of 45.90% alpha helices, 7.38% extended strands, 3.69% beta turns, and 43.03% random coils. Table 6 and Figure 5 present the secondary structural components of cathepsin and mt NADH dhf-2 proteins. The secondary structure of a protein elucidates the conformation of individual amino acids, signifying their arrangement within a helix, strand, or coil. The findings demonstrated that random coils and alpha helices represent the predominant secondary structural elements.

Analysing a protein secondary structure facilitates the examination of hydrogen bonds within the protein, thereby yielding important insights into its structural and functional efficacy. Buxbaum<sup>49</sup> asserts that random coils play a crucial role in proteins by providing flexibility and facilitating conformational changes. Highly flexible glycine and hydrophobic proline amino acids are responsible for the high coil proportion. Proline uniquely induces bends in polypeptide chains, disrupting ordered secondary structures.<sup>50</sup> Neelamathi et al.,<sup>51</sup> indicate that the existence of coiled portions signifies a high degree of preservation and strength in protein structure. Hydrophobic residues create strong interactions with the hydrophobic lipid bilayer when they are added to a mixture.<sup>52</sup> Shelar and Bansal<sup>53</sup> established a correlation between the structures of  $\alpha$ -helical proteins and their diverse activities. These functions include signal detection, receptor activation, ion and chemical transport across membranes, energy transfer, and preservation. Additionally, the elongated conformation of  $\alpha$ -helical proteins may contribute to their dynamic behavior and sliding motion, both of which are essential for their best performances.

**Table 6: Secondary structural elements of cathepsin and mt NADH dhf-2.**

Structural elements	Cathepsin		mt NADH dhf-2	
	No. of residues	% of residues	No. of residues	% of residues
Alpha helices (h)	86	25.75	112	45.90
310 helix (g)	0	0.00	0	0.00
Pi helix (i)	0	0.00	0	0.00
$\beta$ -bridges (b)	0	0.00	0	0.00
Extended strand (e)	51	15.27	18	7.38
$\beta$ -turn (t)	22	6.59	9	3.69

Bend region (s)	0	0.00	0	0.00
Random coil (c)	175	52.40	105	43.03
Ambiguous states	0	0.00	0	0.00
Other states	0	0.00	0	0.00

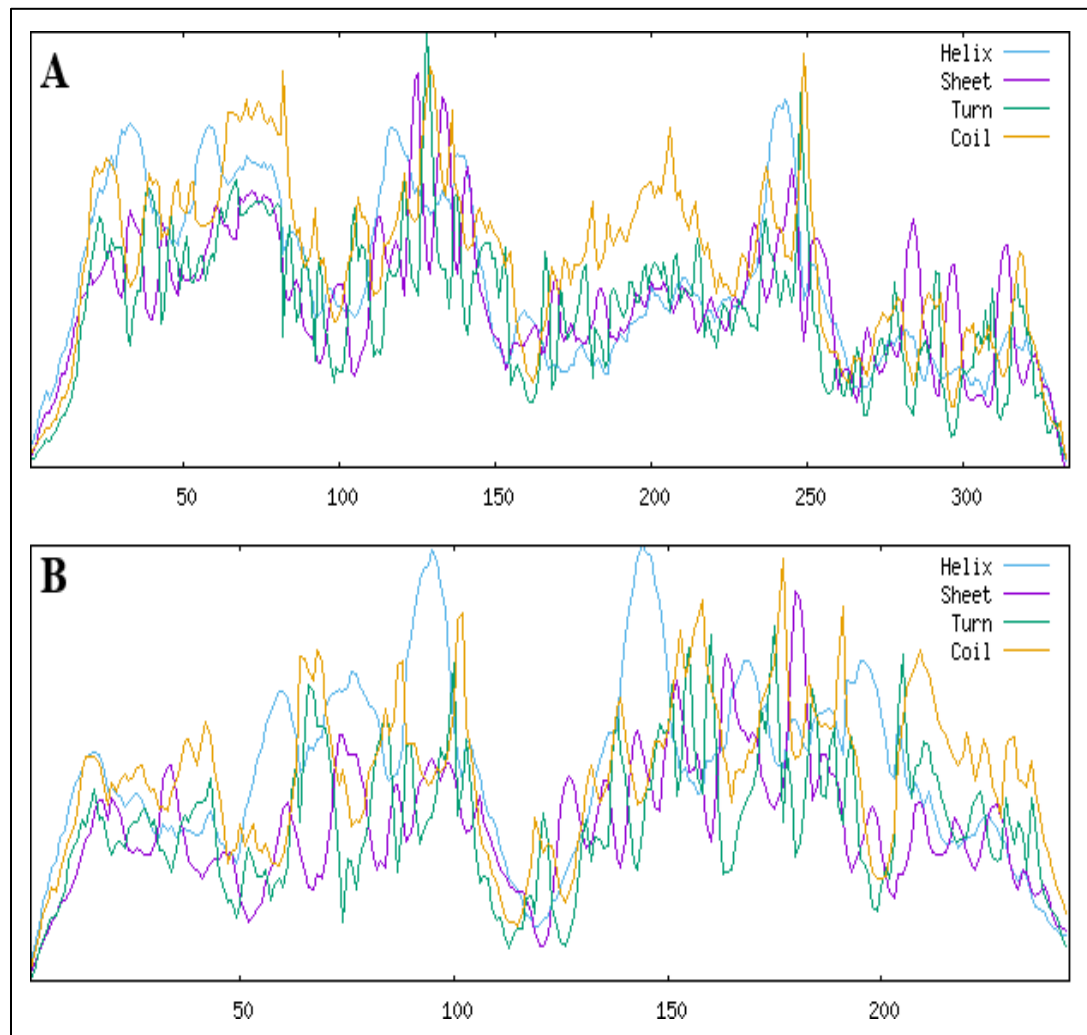


**Figure 5: Spectra of secondary structural elements. A) cathepsin B) mt NADH dhf-2.**

### 3D structure

The 3D models of cathepsin and mt NADH dhf-2 proteins from *G. catla* were predicted using protein IDs C8he9A and C5xtbN as templates, demonstrating identify percentages of 75 and 87% respectively, with a confidence score of 100. Figure 6 and 7 present the predicted 3D representations of cathepsin and mt NADH dhf-2. The confidence score is used to evaluate the accuracy and reliability of predicted structural 3D models. The assessment involves evaluating the threading alignments and convergence parameters of structure assembly simulations.

Homology modelling is a prevalent technique frequently employed in life science research to create structural models of proteins in the absence of available realistic structures. The 3D structure of proteins offers detailed understanding of their interactions and localisation in a stable conformation, and also crucial for their molecular functions. Biasini et al.,<sup>54</sup> asserted that modelling and assessment methods must account for protein flexibility, given that proteins can exist in structurally distinct functional states and are not static entities. The Phyre2 facilitated the generation of 3D structural models for target protein sequences. This method was subsequently utilised to investigate possible folds through threading, using template sequences from the PDB structure database as references.

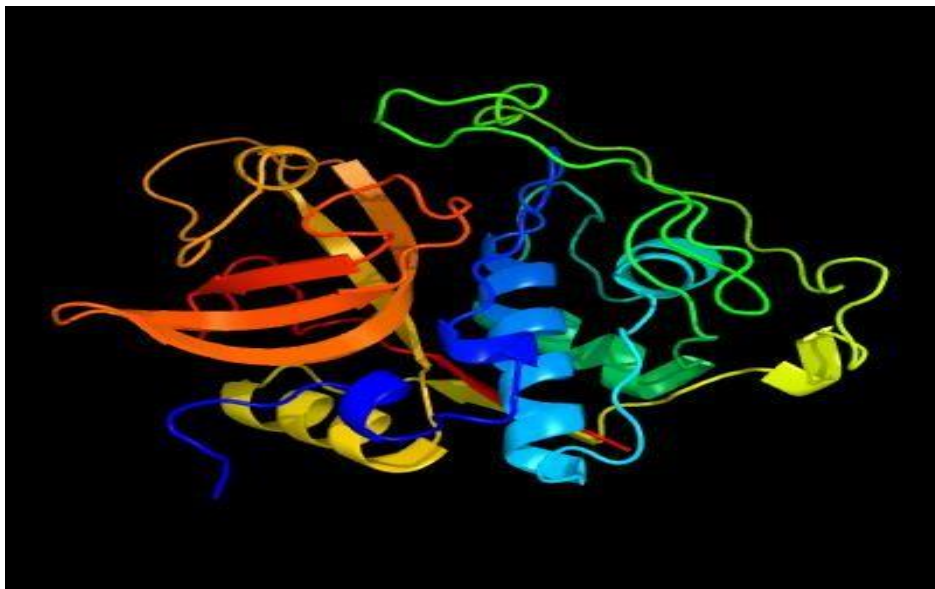


**Figure 6: Predicted 3D model of Cathepsin.**

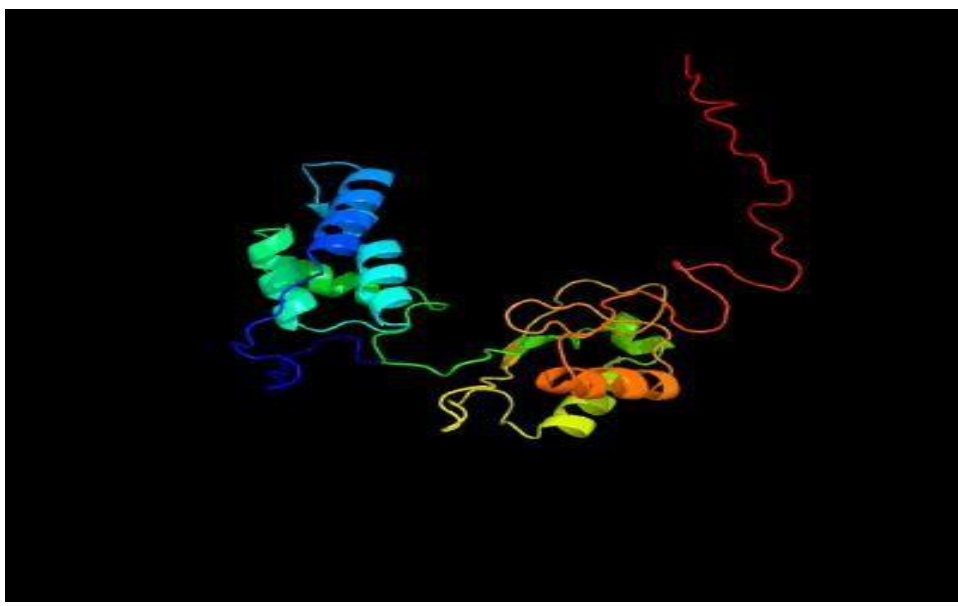


**Figure 7: Predicted 3D model of mt NADH dhf-2.**

#### **Quality assessment of predicted 3D models**

The global quality scores such as QMean,  $c\beta$ , all atoms, solvation, and torsion for the predicted 3D model of cathepsin were predicted as -0.29, -1.76, -3.04, -1.12, and 0.58 respectively. While, the 3D model of mt NADH dhf-2 exhibited the global quality scores of -2.80, 0.34, -0.86, -0.69, and -2.62 for the QMean,  $c\beta$ , all atoms, solvation, and torsion. The predicted models QMEAN score were near zero, signifying high model quality. Figure 8 and 9 presents the density plots and global quality scores of cathepsin and mt NADH dhf-2 3D models. The QMEAN server assessed the accuracy of the predicted 3D models. QMEAN is an index that integrates statistical probabilities of average energy and model reliability with predicted structural properties based on the target protein sequence.<sup>55</sup> Benkert et al.,<sup>56</sup> assert that the effectiveness of the predicted model is contingent upon the QMEAN score, which has been standardised according to the number of interactions.

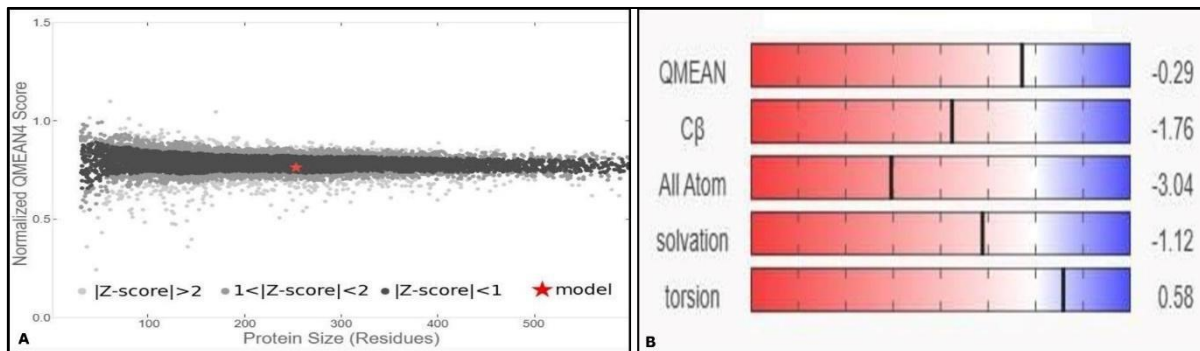


**Figure 8: Plots showing A) QMEAN Z-score B) global quality scores of cathepsin 3D model.**

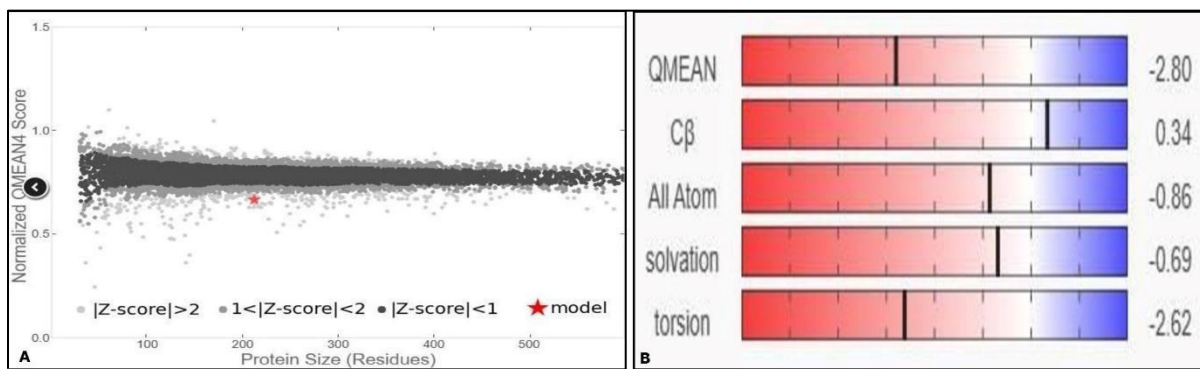


**Figure 9: Plots showing A) QMEAN Z-score B) global quality scores of mt NADH dhf-2 3D model.**

#### Model validation

The structural integrity of the cathepsin and mt NADH dhf-2 proteins 3D models was evaluated using a Ramachandran plot assessment utilising the PROCHECK server, with a particular emphasis on the geometric features of the backbone conformations. The Ramachandran plot for the cathepsin 3D model indicates that 86.6% of residues are situated in the most favoured region, 12.4% in the additionally allowed region, and 1.0% in the generously allowed regions. Figure 10 presents the Ramachandran plot for the predicted 3D model of cathepsin. The Ramachandran plot for the mt NADH dhf-2 model indicates that 81.0% of residues are situated in the most favourable region, 15.5% in the additionally allowed region, 2.3% in the generously allowed region, and 1.1% in the disallowed region. Figure 11 presents the Ramachandran plot for the predicted 3D model of mt NADH dhf-2. Table 7 displays the Ramachandran plot statistics for the cathepsin and mt NADH dhf-2 models. The results indicate that the majority of amino acids phi-psi conformations align with a right-handed helix. The predicted model demonstrates reliability and stability. Based on the idea that the native structure of a protein molecule has the lowest free energy of all its potential conformations, several methods are employed. Kiran et al.,<sup>57</sup> employed PROCHECK to assess the validity of the 3D structure of ATP synthase  $\beta$  and glutamine dependent NAD<sup>+</sup> synthetase.

**Table 7: Ramachandran plot statistics of predicted cathepsin and mt NADH dhf-2 models.**

Residues	Cathepsin		mt NADH dhf-2	
	No. of Residues	% of Residues	No. of Residues	% of Residues
Most favoured regions	175	86.6	141	81.0
Additionally allowed regions	25	12.4	27	15.5
Generously allowed regions	2	1.0	4	2.3
Disallowed regions	0	0	2	1.1

Non-Glycine and Non-Proline	202	100	174	100
End Residues	2	-	0	...
Glycine	33	-	16	...
Proline	16	-	22	...

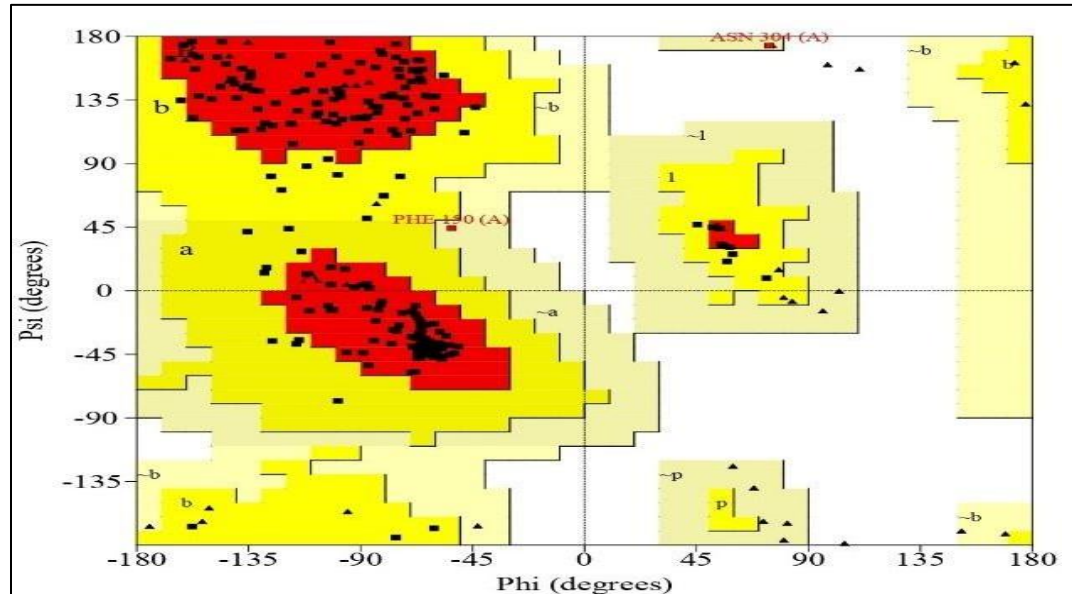


Figure 10: Ramachandran plot statistics of predicted cathepsin structural model.

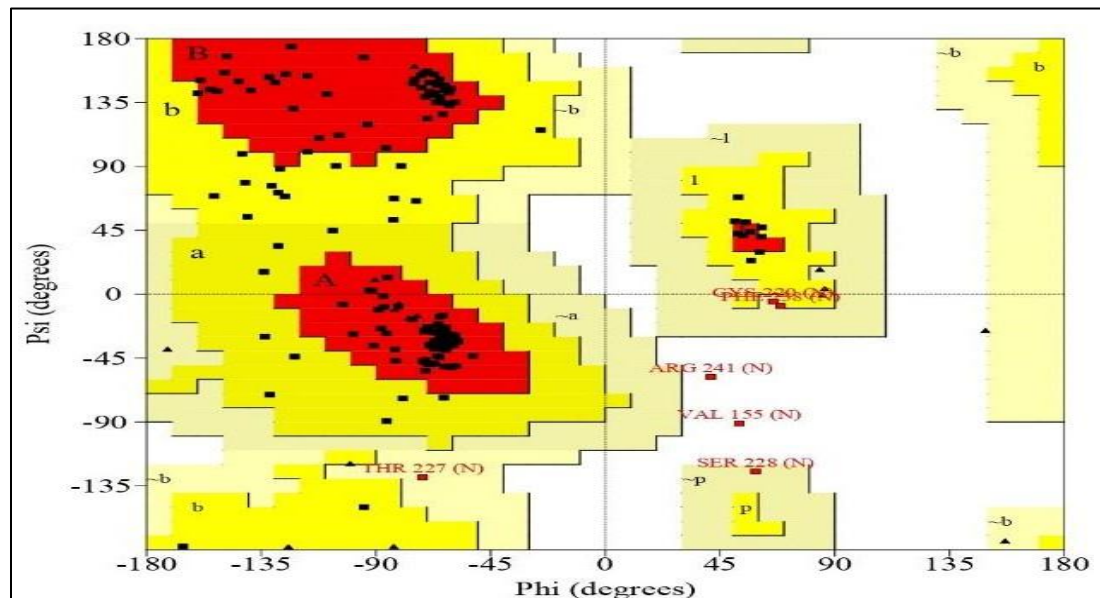


Figure 11: Ramachandran plot statistics of predicted mt NADH dhf-2 structural model.

#### Functional annotations

The functional properties of the cathepsin and mt NADH dhf-2 proteins were predicted in terms of gene ontology terms (GO terms) based on the functional homology score (Fh-score). The 3D model of cathepsin molecular function was associated with the GO:0003824 with a GO score of 0.589, which indicated the catalysis of a biochemical reaction at physiological temperatures. Whereas, the GO terms for biological process of cathepsin was associated with the GO:0009987 with a GO score of 0.644, which indicated the protein is involved in cell physiological process such as cell communication, growth and maintenance. The

cellular component of the cathepsin protein is linked to the GO:0110165 term with a score of 0.688, which indicates that the protein is intracellular.

The 3D model of mt NADH dhf-2 molecular function was associated with the GO:0016491 with a GO score of 0.526, which indicated the protein involved in oxidoreductive reactions. Whereas, the GO terms for biological process of mt NADH dhf-2 was associated with the GO:0008152 with a GO score of 0.672, which indicated the protein is involved in metabolic process include anabolism and catabolism. The cellular component of the mt NADH dhf-2 protein is linked to the GO:0016020 term with a score of 0.689, which indicates that the protein is localised to membrane.

#### PPI network analysis

The STRING database includes protein-protein interactions (PPIs) obtained from both experimental and computational approaches. It assigns a quality score to every interaction by combining data from many sources, including literature and gene expression profiles.<sup>58</sup> The STRING database has comprehensive information on protein biology, including data on their structure, gene sequence, homology, co expression and association. Researchers have processed this data using text mining, computational phylogeny, in vitro, in vivo, and in situ analysis.<sup>59</sup> Analysing the cathepsin and mt NADH dhf-2 proteins with the STRING database, predicted the functional partners of the protein with moderate confidence (score: 0.4). The interaction networks of cathepsin and mt NADH dhf-2 proteins with their predicted functional partners is shown in Figure 12 and 13.

The functional partners of cathepsin were found to be ROHU\_006213 (Dipeptidyl peptidase 1-like protein), ROHU\_006214 (Dipeptidyl peptidase 1-), ROHU\_020112 (Cathepsin Z-like protein), ROHU\_021706 (Cathepsin Z-like protein), ROHU\_014567 (Cathepsin B-like protein), ROHU\_014568 (Cathepsin B-like protein), ROHU\_024770 (Cathepsin B-like protein), ROHU\_003355 (Cathepsin B-like protein), ROHU\_026445 (Cathepsin D), and ROHU\_025240 (Renin-like protein). The statistical parameters of cathepsin such as number of nodes, number of edges, average node degree, average local clustering coefficient, and PPI enrichment P-value in PPI network analysis were found to be 11, 50, 9.09, 0.889, and 1.0e-16.

As well as, the functional partners of mt NADH dhf-2 were found to be ndufs3 (NADH ubiquinone oxidoreductase core subunit S3), ndufs7 (NADH ubiquinone oxidoreductase core subunit S7), ndufs2 (NADH ubiquinone oxidoreductase core subunit S2), ndufv2 (NADH ubiquinone oxidoreductase core subunit V2), ndufa9 (NADH ubiquinone oxidoreductase subunit A9), ndufs4 (NADH ubiquinone oxidoreductase subunit S4), ndufs6 (NADH ubiquinone oxidoreductase subunit S6), ndufa12 (NADH ubiquinone oxidoreductase core subunit A12), LOC114444462 (NADH dehydrogenase 1 beta subcomplex subunit-9), and ndufa10 (NADH ubiquinone oxidoreductase subunit A10). The statistical parameters of mt NADH dhf-2 such as number of nodes, number of edges, average node degree, average local clustering coefficient, and PPI enrichment P-value in PPI network analysis were found to be 11, 55, 10, 1, and 1.0e-16.

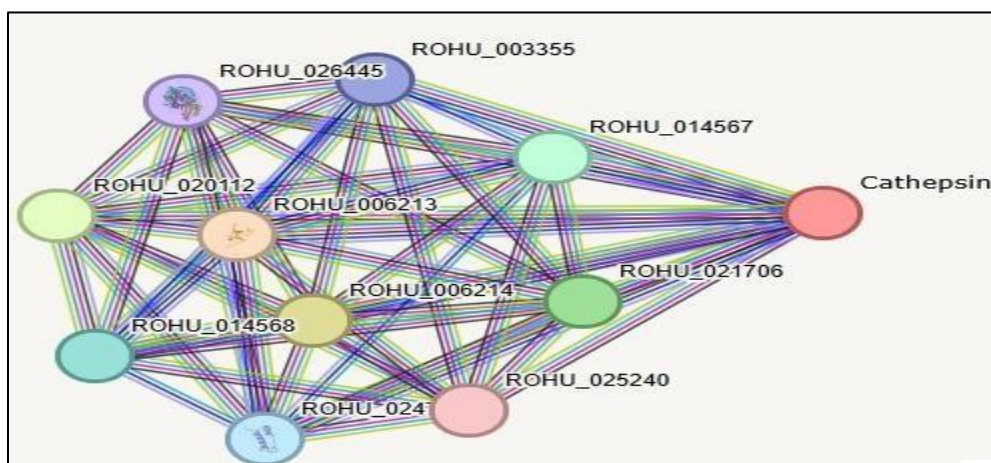
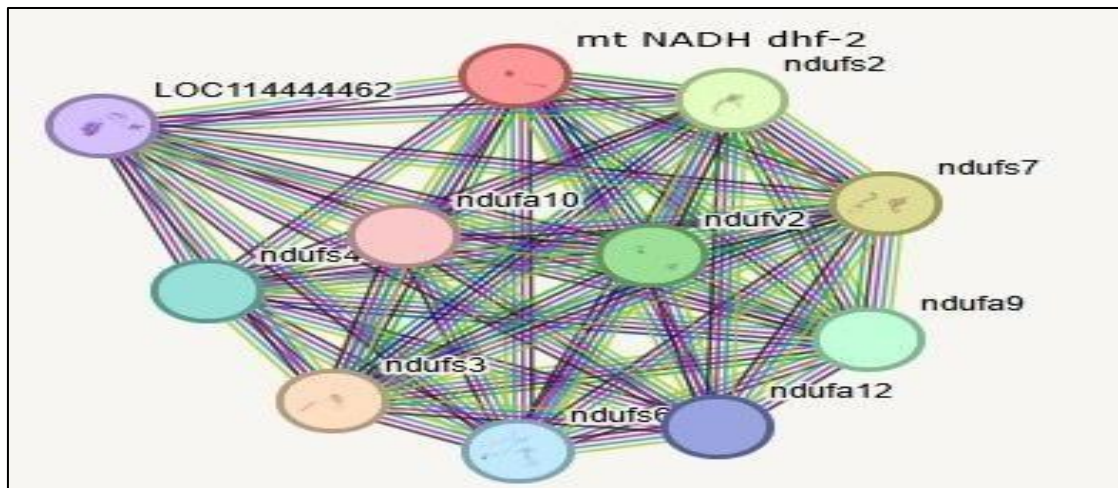


Figure 12: The PPI network of cathepsin and the predicted functional partners.



**Figure 13: The PPI network of mt NADH dhf-2 and the predicted functional partners.**

## CONCLUSION

The research indicated a significant variation in protein content in fish exposed to various dosages of *Aeromonas hydrophila*. Comparative muscle proteome analysis indicated that the majority of protein bands were similar across all the treatment groups. According to the comparative muscle proteome analysis, the majority of the protein bands in each treatment group were identical. Nevertheless, two protein bands with molecular weights recorded at 35 and 28 kDa were additionally found in fish exposed to *A. hydrophila* with 750 and 1000  $\mu$ L/L dosages. These protein bands were recognized as cathepsin and mt NADH dhf-2. The physicochemical characterization indicated that the cathepsin and mt NADH dhf-2 in fish exhibited acidic characteristics, with pI values of 5.58 and 5.70 respectively. The secondary structure analysis revealed that cathepsin and mt NADH dhf-2 exhibit a greater proportion of random coils and alpha helices. Furthermore, the homology modeling showed that the best templates for cathepsin and mtNADH dhf-2 are C8he9A and C5xtbN. Cathepsin and mt NADH dhf-2 predicted models had QMEAN values of -0.29 and -2.80 respectively. The present study showed that the predicted structural models of cathepsin and mt NADH dhf-2 were accurate and coherent.

## Acknowledgement

The authors acknowledge the Department of Zoology, Andhra University, Visakhapatnam, and SSR Biosciences for providing us the laboratory facilities to carry out the research.

## Conflict of interest

The authors declare that there is no conflict of interest.

## REFERENCES

- [1] Chrysanthou, C., Panagiotakos, D. B., Pitsavos, C., Skoumas, J., Krinos, X., Chloptsios, Y., Nikolaou, V., and Stefanidis, C., 2007, "Long-term fish consumption is associated with protection against arrhythmia in healthy persons in a Mediterranean region—the ATTICA study", *The American journal of clinical nutrition*, 85(5), pp. 1385-1391.
- [2] Sujatha, K., Joice, A. A., and Kumaar, P. S., 2013, "Total protein and lipid content in edible tissues of fishes from Kasimedu fish landing centre, Chennai, Tamilnadu", *European Journal of Experimental Biology*, 3(5), pp. 252-257.
- [3] Abraha, B., Admassu, H., Mahmud, A., Tsighe, N., Shui, X. W., and Fang, Y., 2018, "Effect of processing methods on nutritional and physico-chemical composition of fish: a review", *MOJ Food Process Technol.*, 6(4), pp. 376-382.
- [4] Chinabut, S., and Puttinawarat, S., 2005, "The choice of disease control strategies to secure international market access for aquaculture products", *Developmental Biology* (Basal), 121, pp. 255-261.
- [5] Sakai, M., 1999, "Current research status of fish immunostimulants. *Aquaculture*", 172, pp. 63-92.
- [6] Deivasigamani, B., and Subramanian, V., 2016, "Applications of immunostimulants in aquaculture: a review", *Int. J. Curr. Microbiol. App. Sci.*, 5(9), pp. 447-453.
- [7] Xu, X. Y., Shen, Y. B., Fu, J. J., Liu, F., Guo, S. Z., Yang, X. M., and Li, J. L., 2012, "Matrix metalloproteinase 2 of grass carp *Ctenopharyngodon idella* (CiMMP2) is involved in the immune response against bacterial infection", *Fish & shellfish immunology*, 33(2), pp. 251-257.
- [8] Adams, S. M., 2005, "Assessing cause and effect of multiple stressors on marine systems", *Mar. Pollut. Bull.*, 51, pp. 649-657.

[9] Adah, A. D., Saidu, L., Oniye, S. J., Kazeem, H. M., and Adah, S. A., 2021, "Prevalence and risk factors Associated with *Aeromonas hydrophila* Infection in *Clarias gariepinus* and Pond Water from Fish farms in Kaduna State Nigeria", *Jordan J Biol Sci.*, 14(3), 477-84. <https://doi.org/10.54319/jjbs/140313>.

[10] Viarengo, A., Lowe, D., Bolognesi, C., Fabbri, E., and Koehler, A., 2007, "The use of biomarkers in biomonitoring: A 2-tier approach assessing the level of pollutant-induced stress syndrome in sentinel organisms", *Comp. Biochem. Physiol. C Toxicol. Pharmacol.*, 146, pp. 281-300.

[11] Casanovas, P., Walker, S., Johnston, H., Johnston, C., and Symonds, J., 2021, "Comparative assessment of blood biochemistry and haematology normal ranges between Chinook salmon (*Oncorhynchus tshawytscha*) from seawater and freshwater farms", *Aquaculture*, 537, pp. 736464.

[12] Harikrishnan, R., Balasundaram, C., and Heo, M. S., 2011, "Fish health aspects in grouper aquaculture", *Aquaculture*, 320(1-2), pp. 1-21. <https://doi.org/10.1016/j.aquaculture.2011.07.022>.

[13] Foran, C. M., and Bass, A. H., 1999, "Preoptic GnRH and AVT: axes for sexual plasticity in teleost fish", *General and comparative endocrinology*, 116(2), pp. 141-152. <https://doi.org/10.1006/gcen.1999.7357>.

[14] Garlov, P. E., 2005, "Plasticity of nonapeptidergic neurosecretory cells in fish hypothalamus and neurohypophysis", *International review of cytology*, 245, pp. 123-170. [https://doi.org/10.1016/S0074-7696\(05\)45005-6](https://doi.org/10.1016/S0074-7696(05)45005-6).

[15] Godwin, J., and Thompson, R., "Nonapeptides and social behavior in fishes", *Hormones and Behavior*, 61(3), pp. 230-238. <https://doi.org/10.1016/j.yhbeh.2011.12.016>.

[16] Lowry, O. H., Rosebrough, N. J., Farr, A. L., and Randall, R. J., "Protein measurement with the Folin phenol reagent", *J biol Chem.*, 193(1), pp. 265-275.

[17] Sambrook, J., and Russell, D. W., 2001, "Molecular Cloning: In Vitro amplification of DNA by the polymerase chain reaction", *Cold Spring Harbor Laboratory Press*, 2, Chap. 8.

[18] Laemmli, U. K., 1970, "Cleavage of structural proteins during the assembly of the head of bacteriophage T4", *Nature*, 227(5259), pp. 680-685. <https://doi.org/10.1038/227680a0>.

[19] Bairoch, A., and Apweiler, R., 2000, "The SWISS-PROT protein sequence database and its supplement TrEMBL in 2000", *Nucleic acids research*, 28(1), pp. 45-48. doi: 10.1093/nar/28.1.45.

[20] Kelley, L. A., Mezulis, S., Yates, C. M., Wass, M. N., and Sternberg, M. J., 2015, "The Phyre2 web portal for protein modeling, prediction and analysis", *Nature protocols*, 10(6), pp. 845-858. <https://doi.org/10.1038/nprot.2015.053>.

[21] Ali, M., Salam, A., and Iqbal, F., 2001, "Effect of environmental variables on body composition parameters of *Channa punctata*", *Journal of Research Science*, 12(2), pp. 200-206.

[22] Adawayah, R., 2007, "Pengolahan dan Pengawetan Ikan", Jakarta: Bumi Aksara.

[23] Dabholade, V. F., Pathan, T. S., Shinde, S. E., Bhandare, R. Y., and Sonawane, D. L., 2009, "Seasonal variations of protein in the ovary of fish *Channa gachua*", *Recent Research in Science and Technology*, 1(2), pp. 078-080.

[24] Satyalatha, D. J., and Viveka, V., 2014, "Aeromoniasis Induced Protein and DNA and Histological Alterations in the muscle tissues of *Labeo rohita*", *IOSR Journal of Pharmacy and Biological Sciences.*, 9, pp. 107-111. 10.9790/3008-0942107111.

[25] Karunasagar, I., Rosalind, G., and Karunasagar, I., 1991, "Immunological responses of the Indian major carps to *Aeromonas hydrophila* vaccine", *J. Fish. Dis.*, 14, pp. 413-417.

[26] Lamers, C. H. J., and Van Muiswinkel, W. B., 1986, "Natural and acquired agglutinin to *Aeromonas hydrophila* in carp *Cyprinus carpio*", *Can. J. Fish. Aquat. Sci.*, 43, pp. 619-624.

[27] Newman, S. G., 1993, "Bacterial vaccines for fish", *Ann. Rev. Fish Dis.*, 3, pp. 145-185.

[28] Begum, G., 2004, "Carbofuran insecticide induced biochemical alterations in liver and muscle tissues of the fish *Clarias batrachus* (Linn.) and recovery response", *Aquatic Toxicol.*, 66(1), pp. 83-92.

[29] Miyamoto, J., 1976, "Degradation metabolism and toxicity of synthetic pyrethroid", *Environ. Health Perspect.*, 14, pp. 15-28.

[30] Murty, A. S., and Devi, A. P., 1982, "The Effect of Endosulfan and its Isomers on Tissue Protein, Glycogen and Lipids in the fish *Channa punctata*", *Pestl. Biochem. Physiol.*, 17, pp. 280-286.

[31] Das, S., and Bhattacharya, T., 2006, "Impact of Water Pollution on Fish Physiology – A Study", *J. Aquaculture*, 14, pp. 1-16.

[32] Neilson, S., 1975, "Osmoregulation. Effect of salinities and heavy metal", *Fed. Proc.*, 33, pp. 2137-2146.

[33] Veeraiah, K., and Durga Prasad, M. K., 1998, "Study on the toxic effects of cypermethrin (technical) on organic constituents of freshwater fish, *Labeo rohita*", *Proc. Acad. Environ. Biol.*, 7(2), pp. 143-148.

[34] Durairaj, S., and Selvarajan, V. R., 1992, "Influence of Quinolophos, an organophosphorus pesticide on the biochemical constituents of the tissues of fish, *Oreochromis mossambicus*", *J. Environ. Biol.*, 13(3), pp. 181-185.

[35] Dawar, F. U., Tu, J., Xiong, Y., Lan, J., Dong, X. X., Liu, X., Khattak, M. N., Mei, J., and Lin, L., 2016, "Chemotactic activity of cyclophilin a in the skin mucus of yellow catfish (*Pelteobagrus fulvidraco*) and its active site for chemotaxis", *International journal of molecular sciences.*, 17(9), pp. 1422.

[36] Ali, S., Dawar, F. U., Ullah, W., Hassan, M., Ullah, K., and Zhao, Z., 2023, "Proteomic map of the differentially expressed proteins in the skin of *Ctenopharyngodon idella* against *Aeromonas hydrophila* infection", *Fish and Shellfish Immunology*, Reports., 5, pp. 100122.

[37] Canellas, A. L. B., Costa, W. F., Freitas-Silva, J., Lopes, I. R., de Oliveira, B. F. R., and Laport, M. S., 2022, "In sickness and in health: Insights into the application of omics in aquaculture settings under a microbiological perspective", *Aquaculture*, 554, pp. 738132.

[38] Lu, A., Hu, X., Wang, Y., Shen, X., Li, X., Zhu, A., Tian, J., Ming, Q., and Feng, Z., 2014, "iTRAQ analysis of gill proteins from the zebrafish (*Danio rerio*) infected with *Aeromonas hydrophila*", *Fish & shellfish immunology*, 36(1), pp. 229-239. <https://doi.org/10.1016/j.fsi.2013.11.007>.

[39] Lu, A., Hu, X., Xue, J., Zhu, J., Wang, Y., and Zhou, G., 2012, "Gene expression profiling in the skin of zebrafish infected with *Citrobacter freundii*", *Fish & shellfish immunology*. 32(2), pp. 273-83.

[40] Zaccone, G., Fasulo, S., Ainis, L., and Contini, A., 1989, "Localization of calmodulin positive immunoreactivity in the surface epidermis of the brown trout, *Salmo trutta*", *Histochemistry*. 91(1), pp. 13-16.

[41] Dash, S., Das, S. K., Samal, J., and Thatoi, H. N., 2018, "Epidermal mucus, a major determinant in fish health: a review", *Iranian journal of veterinary research*. 19(2), pp. 72.

[42] Wang, L., Shao, C., Xu, W., Zhou, Q., Wang, N., and Chen, S., 2017, "Proteome profiling reveals immune responses in Japanese flounder (*Paralichthys olivaceus*) infected with *Edwardsiella tarda* by iTRAQ analysis", *Fish & Shellfish Immunology*., 66: pp. 325-33.

[43] Mann, M., Hendrickson, R. C., and Pandey, A., 2001, "Analysis of proteins and proteomes by mass spectrometry", *Annual review of biochemistry*. 70(1), pp. 437-473. <https://doi.org/10.1146/annurev.biochem.70.1.437>.

[44] Guruprasad, K., Reddy, B. B., and Pandit, M. W., 1990, "Correlation between stability of a protein and its dipeptide composition: a novel approach for predicting in vivo stability of a protein from its primary sequence", *Protein Engineering, Design and Selection*. 4(2), pp. 155-161. <https://doi.org/10.1093/protein/4.2.155>.

[45] Zaccaria, D., Greco, R., Bozzaro, S., Ceccarelli, A., and MacWilliams, H., 1998, "UGUS, a reporter for use with destabilizing N-termini", *Nucleic acids research*. 26(4), pp. 1128-1129. <https://doi.org/10.1093/nar/26.4.1128>.

[46] Rogers, S., Wells, R., and Rechsteiner, M., 1986, "Amino acid sequences common to rapidly degraded proteins: the PEST hypothesis", *Science*. 234(4774), pp. 364-368. doi: 10.1126/science.2876518.

[47] Ikai, A., 1980, "Thermostability and aliphatic index of globular proteins", *J. Biochem.*, 88, pp. 1895–1898.

[48] Kyte, J., and Doolittle, R. F., "A simple method for displaying the hydropathic character of a protein", *J. Mol. Biol.*, 157, pp. 105–132.

[49] Buxbaum, E., 2007, "Fundamentals of protein structure and function", Springer, New York, 31.

[50] Vidhya, V. G., Upgade, A., Bhaskar, A., and Deb, D., 2012, "in silico characterization of bovine (Bos taurus) antiapoptotic proteins", *J Proteins Proteom.*, 3(3), pp. 187-196.

[51] Neelamathi, E., Vasumathi, E., Bagyalakshmi, S., and Kannan, R., 2009, "in silico prediction of structure and functional aspects of a hypothetical protein of *Neurospora crassa*", *Journal of Cell and Tissue Research*., 9(3), pp. 1989.

[52] Ulmschneider, M. B., and Sansom, M. S., 2001, "Amino acid distributions in integral membrane protein structures", *Biochimica et Biophysica Acta (BBA)-Biomembranes*., 1512(1), pp. 1-14. [https://doi.org/10.1016/S0005-2736\(01\)00299-1](https://doi.org/10.1016/S0005-2736(01)00299-1).

[53] Shelar, A., and Bansal, M., 2014, "Sequence and conformational preferences at termini of  $\alpha$ -helices in membrane proteins: Role of the helix environment", *Proteins: Structure, Function, and Bioinformatics*. 82(12), pp. 3420-3436. <https://doi.org/10.1002/prot.24696>.

[54] Biasini, M., Bienert, S., Waterhouse, A., Arnold, K., Studer, G., Schmidt, T., Kiefer, F., Cassarino, T. G., Bertoni, M., Bordoli, L., and Schwede, T., 2014, "SWISS-MODEL: modelling protein tertiary and quaternary structure using evolutionary information", *Nucleic acids research*. 42(W1), pp. W252-W258. doi: 10.1093/nar/gku340.

[55] Sippl, M. J., 1993, "Recognition of errors in three-dimensional structures of proteins", *Proteins: Structure, Function, and Bioinformatics*. 17(4), pp. 355-362. <https://doi.org/10.1002/prot.340170404>.

[56] Benkert, P., Biasini, M., and Schwede, T., 2011, "Toward the estimation of the absolute quality of individual protein structure models", *Bioinformatics*. 27(3), pp. 343-350. doi: 10.1093/bioinformatics/btq662.

[57] Kiran, M. K., Sandeep, B. V., and Sudhakar, P., 2020, "Identification and in-silico characterization of differentially expressed salt-induced proteins in the leaves of mangrove grass *Myriostachya wightiana*", *Journal of Applied Biology & Biotechnology*., 8(05), pp. 48-58. doi: 10.7324/JABB.2020.80506.

[58] Szklarczyk, D., Morris, J. H., Cook, H., Kuhn, M., Wyder, S., Simonovic, M., Santos, A., Doncheva, N. T., Roth, A., Bork, P., and Jensen, L. J., 2016. "The STRING database in 2017: quality-controlled protein–protein association networks, made broadly accessible", *Nucleic acids research*. pp. gkw937 <https://doi.org/10.1093/nar/gkw937>.

[59] Szklarczyk, D., Gable, A. L., Lyon, D., Junge, A., Wyder, S., Huerta-Cepas, J., Simonovic, M., Doncheva, N. T., Morris, J. H., Bork, P., and Jensen, L. J., 2019, "STRING v11: protein–protein association networks with increased coverage, supporting functional discovery in genome-wide experimental datasets", *Nucleic acids research*., 47(D1), pp. D607-D613. <https://doi.org/10.1093/nar/gky1131>.